

Electronic Supplementary Information for

Excited state dynamics of BODIPY-based acceptor-donor-acceptor systems: a combined experimental and computational study

Zimu Wei,[†] Sushil Sharma,[‡] Abbey M. Philip,[†] Sanchita Sengupta,[‡] Ferdinand C. Grozema^{†}*

[†] Department of Chemical Engineering, Delft University of Technology, Delft, The Netherlands.

[‡] Department of Chemical Sciences, Indian Institute of Science Education and Research (IISER) Mohali, Punjab-140306, India.

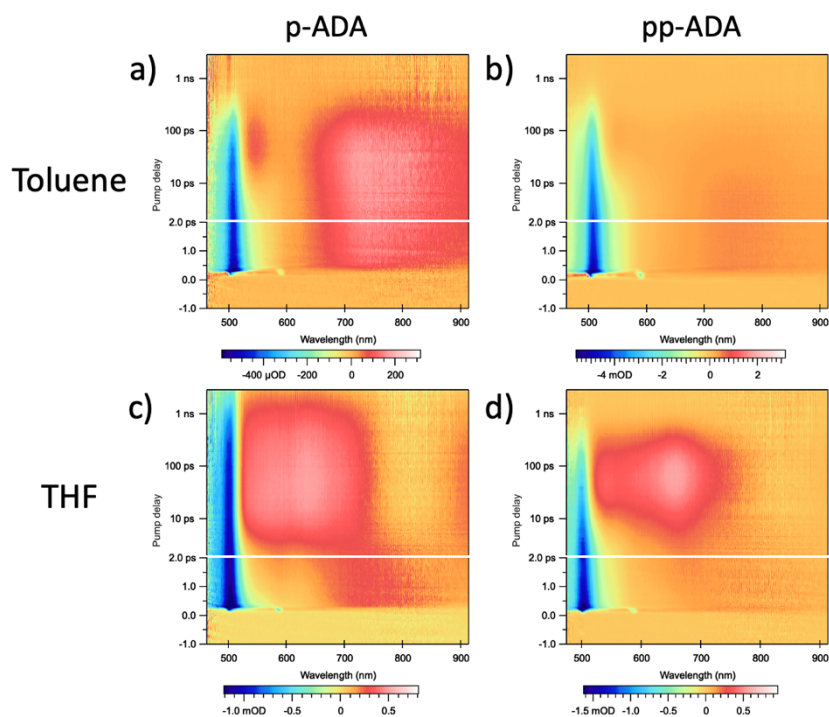


Figure S1. Contour plots of the transient absorption spectra of **p-ADA** and **pp-ADA** in toluene and THF with photoexcitation at 500 nm.

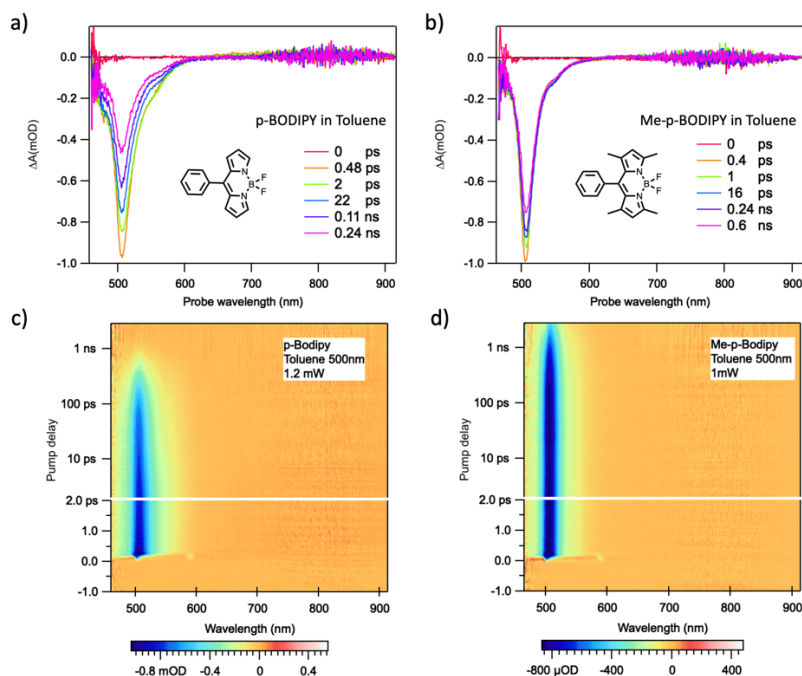


Figure S2. Transient absorption spectra and their contour plots of a), c) **p-BODIPY** and b), d) **Me-p-BODIPY** in toluene with photoexcitation at 500 nm.

Table S1. Adiabatic electron affinity of **p-BODIPY** and **Me-p-BODIPY** calculated by DFT

	E_{bonding} (neutral)	E_{bonding} (negative)	E_{EA}
p-BODIPY	-290.0297 eV	-292.2175 eV	2.19 eV
Me-p-BODIPY	-380.3387 eV	-382.0885 eV	1.75 eV

Geometries of the neutral molecule and the negatively charged molecule were optimized by DFT calculations with CAM-B3LYP/DZP to obtain the total bonding energy, E_{bonding} , of the molecules. The adiabatic electron affinity, E_{EA} , is calculation by

$$E_{\text{EA}} = E_{\text{bonding}}(\text{neutral}) - E_{\text{bonding}}(\text{negative})$$

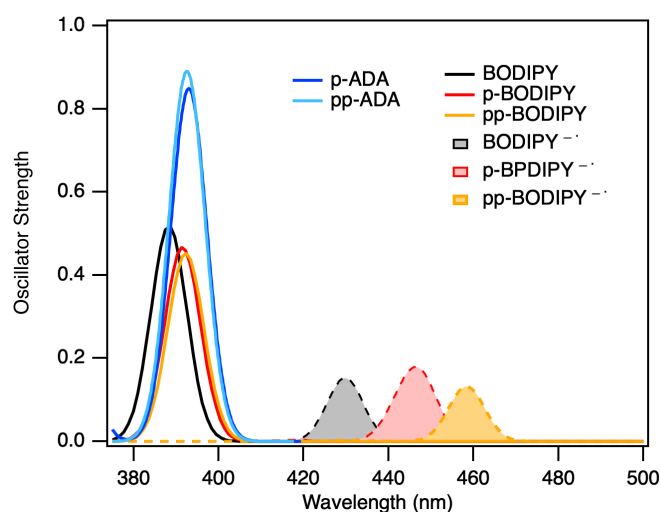


Figure S3. Vertical transition energies calculated by TDDFT with CAM-B3LYP/DZP.

According to the TDDFT calculations, the lowest allowed transitions in both **p-ADA** and **pp-ADA** are located at ~393 nm. Their oscillator strengths are nearly twice as large as these of the individual acceptors, in line with the incorporation of two acceptors in triad molecules. **p-ADA**, **pp-ADA** and **p-BODIPY** show similar vertical transition energies, which is in consistent with

their overlapping experimental absorption spectra, showing the strength of the calculations. For the neutral BODIPY molecules, increasing the number of phenyl units has a small impact on the lowest excitation energy. For the negatively charged BODIPY molecules, the excitation energy is systematically red-shifted by dozens of nanometers with the increasing the number of phenyl units. This possibly associated with the transformation of the two broad absorption features at 580 nm and 635 nm of the CT state in **p-ADA** into the one sharp absorption peak at 658 nm of that in **pp-ADA**.

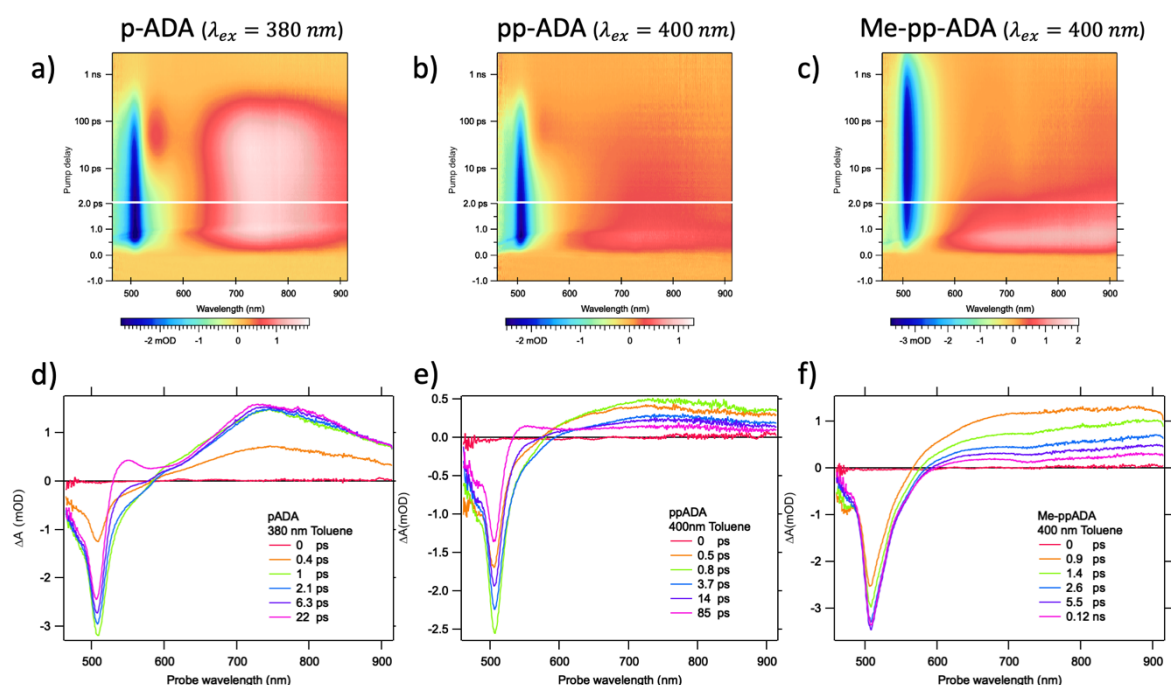


Figure S4. Transient absorption spectra and their contour plots of ADA triads in toluene with photoexcitation at 380/400 nm.

In general, the TA spectrum of **p-ADA** in toluene (Figure S4a) is similar to that at the excitation of acceptor (Figure S1a). Nevertheless, in the first picosecond, the GSB at ~ 500 nm is growing to the maximum instead of simultaneously reaching the maximum upon the photoexcitation. Meanwhile, the broad ESA band experiences a narrowing in the band width and a growth in

the amplitude, giving rising to the spectral signature of the excited acceptor. These features indicate an ultrafast excitation energy transfer from the BDT donor to the BODIPY acceptor. In **pp-ADA**, the absorption band between 650 nm and 900 nm is less pronounced than that in **p-ADA**, consistent with the weaker ESA of acceptor in **pp-ADA**. Since no ESA of acceptor is observed in **Me-pp-ADA** as indicated in Figure 3c, Figure S4f further demonstrates that the broad absorption band presented upon the excitation is associated with the absorption of the excited donor.

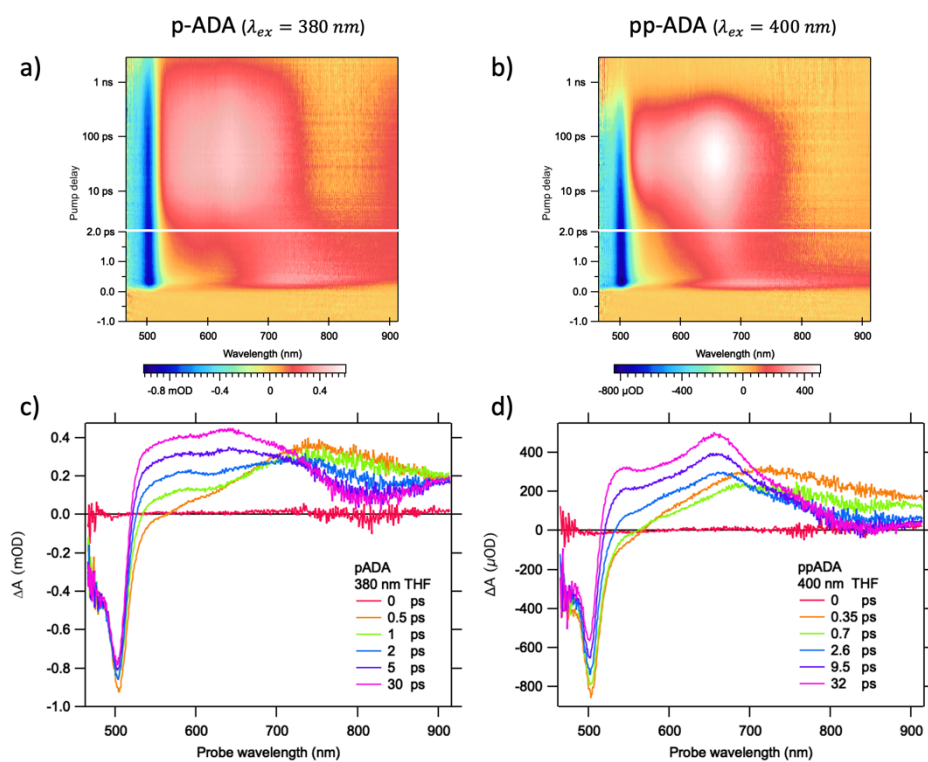


Figure S5. Transient absorption spectra and their contour plots of **p-ADA** and **pp-ADA** in THF with photoexcitation at 380/400 nm.

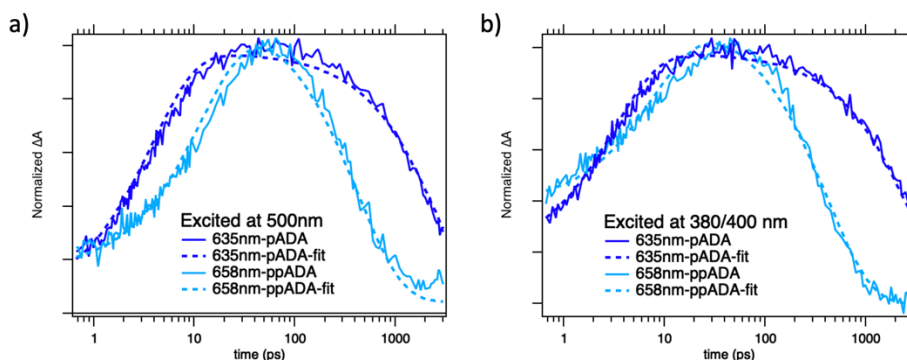


Figure S6. Selected time traces (solid lines) and fits (dashed lines) at the characteristic wavelengths of the charge transfer state for **p-ADA** (dark blue) and **pp-ADA** (light blue).

Table S2. Time constants of global analysis of the TA spectra and fluorescence lifetime

		THF		Toluene	
		p-ADA	pp-ADA	p-ADA	pp-ADA
Excited at 500 nm	τ_1	3.83 ps	11.65 ps	7.83 ps	14.0 ps
	τ_2	2.68 ns	0.44 ns	0.25 ns	0.3 ns
Excited at 380/400 nm	τ_1	3.24 ps	8.38 ps	11.1 ps	14.5 ps
	τ_2	2.80 ns	0.42 ns	0.27 ns	0.26 ns
Excited at 404 nm	τ_{FL}	2.44 ns @660nm	0.46 ns @725nm	0.32 ns (76%) 1.80 ns (24%) @540nm	0.34 ns (80%) 1.27 ns (20%) @530nm

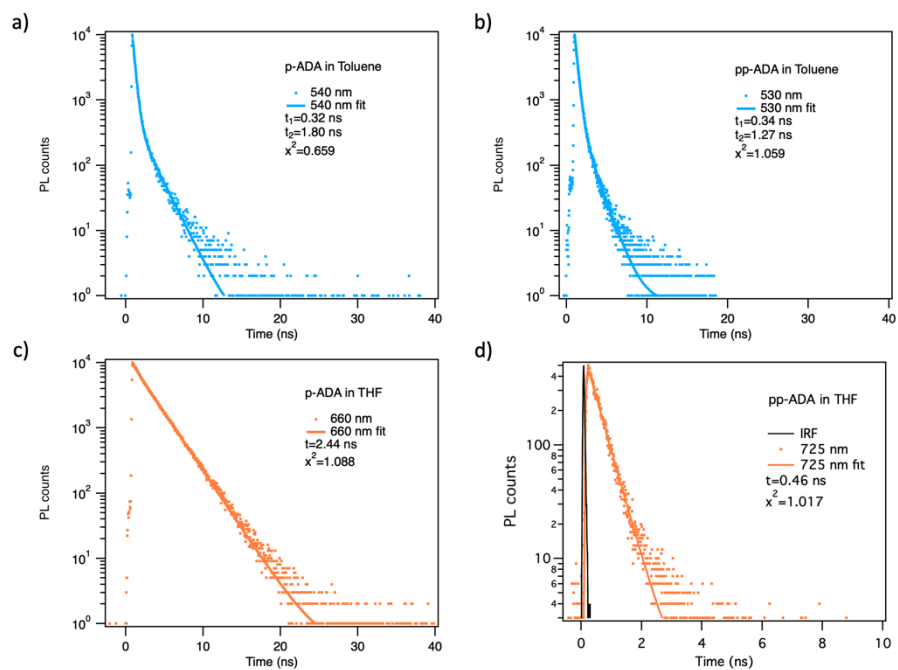


Figure S7. Fluorescence lifetime recorded at different wavelengths excited at 404 nm for **p-ADA** a) in toluene and c) in THF, and for **pp-ADA** b) in toluene and d) in THF.

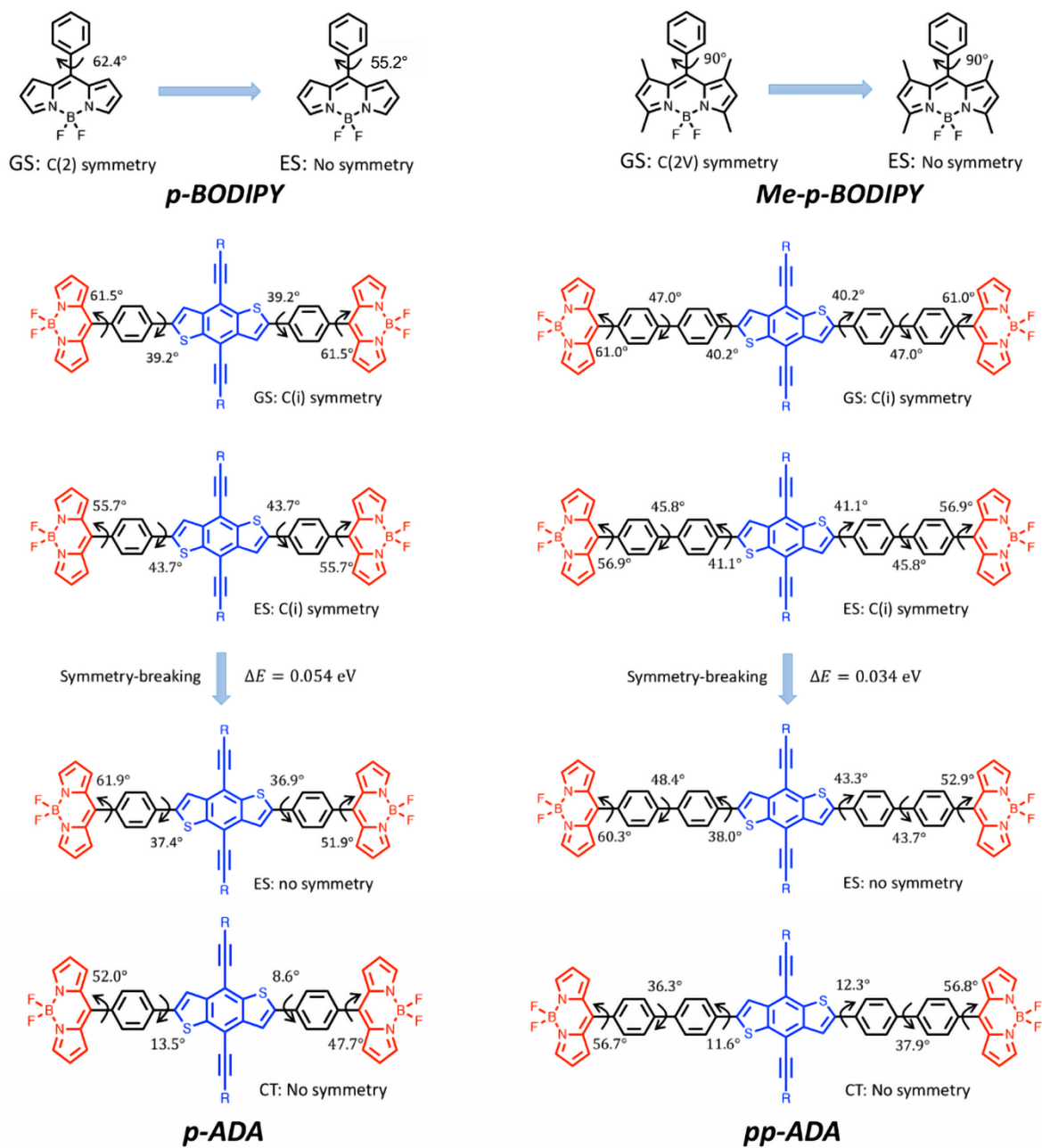


Figure S8. Torsion angles in the geometry optimized ground state (GS), symmetrical excited state (ESSym), asymmetrical excited state (ES) and charge transfer state (CT) of **p-ADA** and **pp-ADA** and BODIPY-Ph torsion angles in GS and ES of **p-BODIPY** and **Me-p-BODIPY**.

Table S3. Major single orbital transitions for the lowest allowed transition of **p-ADA** with geometries of optimized ground state (GS), symmetrical excited state (ES_{sym}), asymmetrical excited state (ES) and charge transfer state (CT).

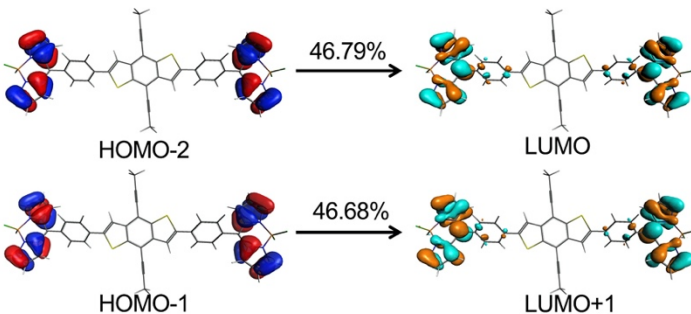
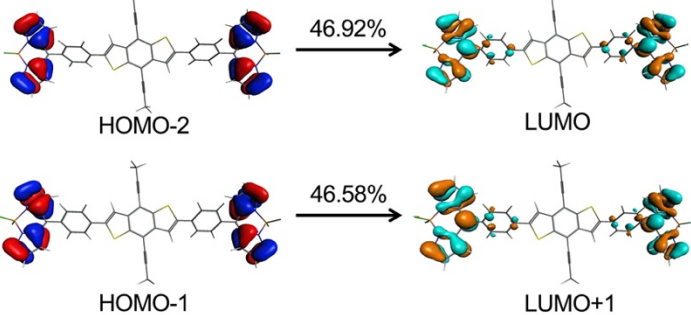
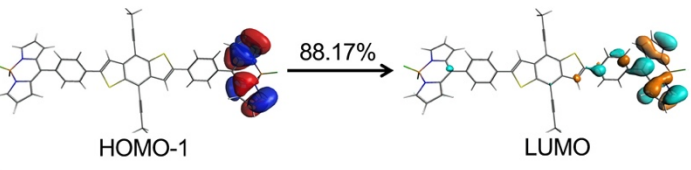
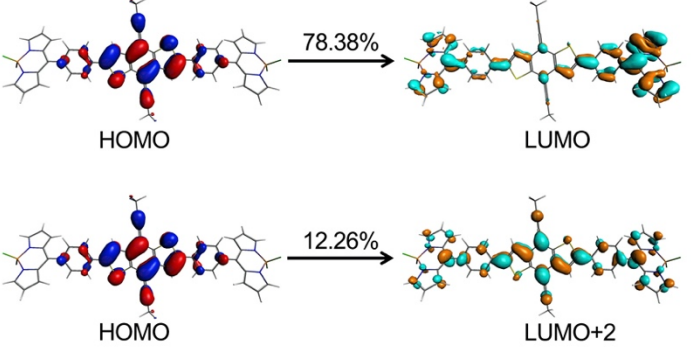
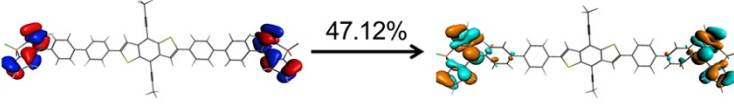
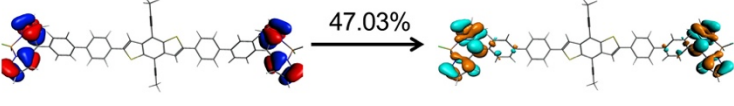
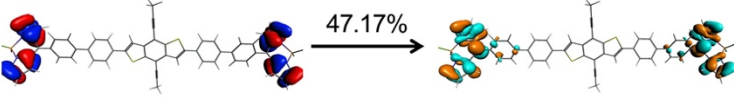
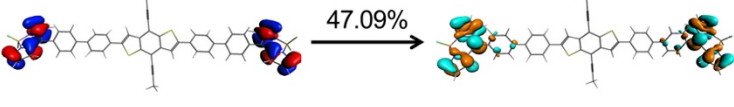
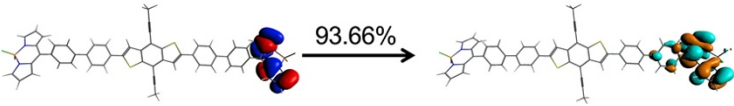
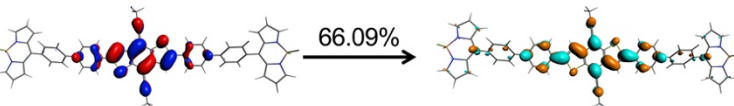
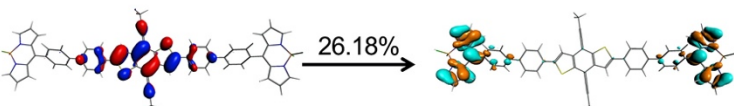
Geometry	Excitation Energy/ Oscillator Strength	Major MO -> MO transitions for the lowest allowed excitation
GS	3.155 eV/ 0.85	 <p>HOMO-2 → LUMO (46.79%)</p> <p>HOMO-1 → LUMO+1 (46.68%)</p>
ES _{sym}	3.089 eV/ 0.80	 <p>HOMO-2 → LUMO (46.92%)</p> <p>HOMO-1 → LUMO+1 (46.58%)</p>
ES	2.977 eV/ 0.35	 <p>HOMO-1 → LUMO (88.17%)</p>
CT	2.737 eV/ 1.62	 <p>HOMO → LUMO (78.38%)</p> <p>HOMO → LUMO+2 (12.26%)</p>

Table S4. Major single orbital transitions for the lowest allowed transition of **pp-ADA** with geometries of optimized ground state (GS), symmetrical excited state (ES_{sym}), asymmetrical excited state (ES) and charge transfer state (CT).

Geometry	Excitation Energy/ Oscillator Strength	Major MO -> MO transitions for the lowest allowed excitation
GS	3.159 eV/ 0.89	 <p>HOMO-2 → LUMO+1 (47.12%)</p>  <p>HOMO-1 → LUMO (47.03%)</p>
ES _{sym}	3.096 eV/ 0.84	 <p>HOMO-2 → LUMO+1 (47.17%)</p>  <p>HOMO-1 → LUMO (47.09%)</p>
ES	3.008 eV/ 0.38	 <p>HOMO-1 → LUMO (93.66%)</p>
CT	2.885 eV/ 2.03	 <p>HOMO → LUMO+2 (66.09%)</p>  <p>HOMO → LUMO (26.18%)</p>

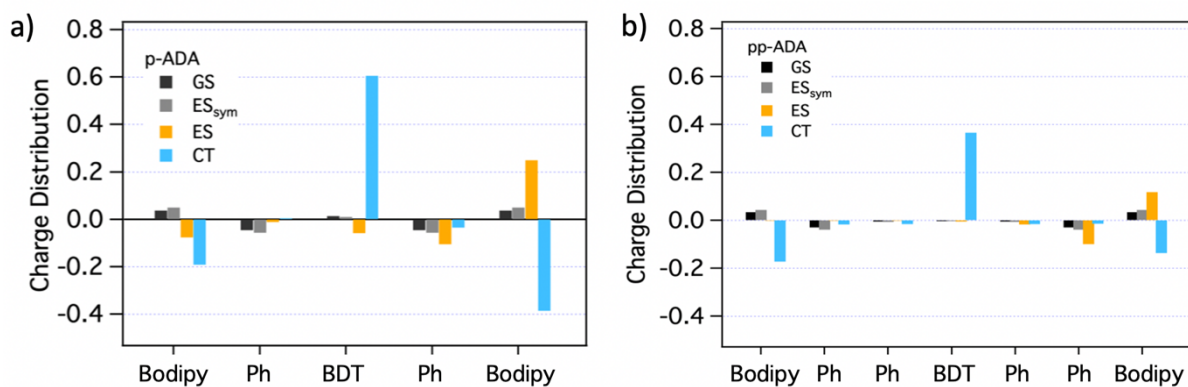


Figure S9. Geometry-dependent charge distribution over the BODIPY acceptors, the individual phenyl units and the BDT donor of the excited state as compared to the ground-state corresponding to the lowest vertical transition for a) p-ADA and b) pp-ADA. Only the single orbital transitions with contribution larger than 1% are taken into account.

Table S5. State-specific solvent stabilization of the local excited state and charge-transfer state in **p-ADA** and **pp-ADA**.

		p-ADA			
		E_{vacuum}	E_{THF}	ΔE	$\Delta E_{\text{solvent}}$
ES geometry	GS	-816.3083 eV	-816.9700 eV	0.662 eV	0.053 eV
	HOMO-1→LUMO	-813.4458 eV	-814.1607 eV	0.715 eV	
CT geometry	GS	-816.1006 eV	-816.7846 eV	0.684 eV	0.735 eV
	HOMO→LUMO	-813.628 eV	-815.0474 eV	1.419 eV	
		pp-ADA			
		E_{vacuum}	E_{THF}	ΔE	$\Delta E_{\text{solvent}}$
ES geometry	GS	-1003.4718 eV	-1004.1925 eV	0.721 eV	0.022 eV
	HOMO-1→LUMO	-1000.5769 eV	-1001.3203 eV	0.743 eV	
CT geometry	GS	-1003.2479 eV	-1003.9853 eV	0.737 eV	1.252 eV
	HOMO→LUMO	-999.8068 eV	-1001.7956 eV	1.989 eV	

E_{vacuum} : Total bonding energy in vacuum; E_{THF} : Total bonding energy in THF; $\Delta E = E_{\text{vacuum}} - E_{\text{THF}}$; $\Delta E_{\text{solvent}}$: Solvent stabilization energy.

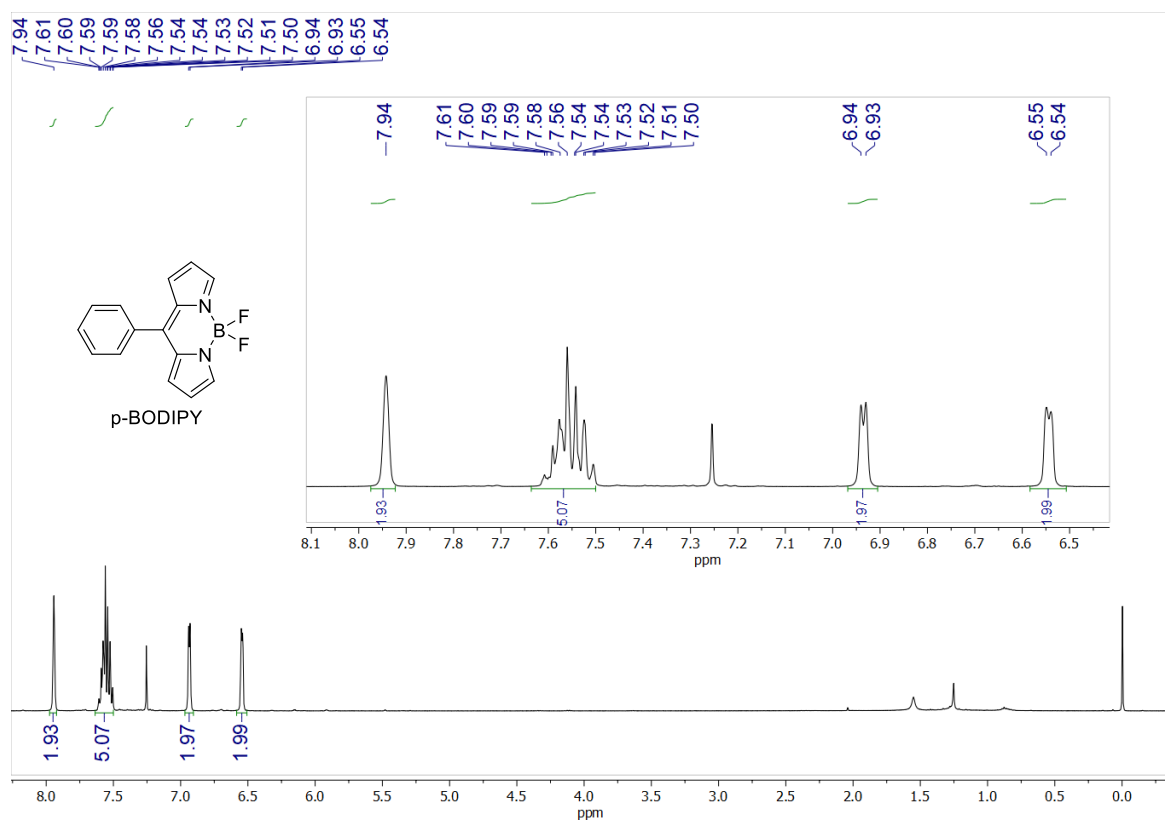


Figure S10. ¹H NMR spectrum of p-BODIPY in CDCl₃.

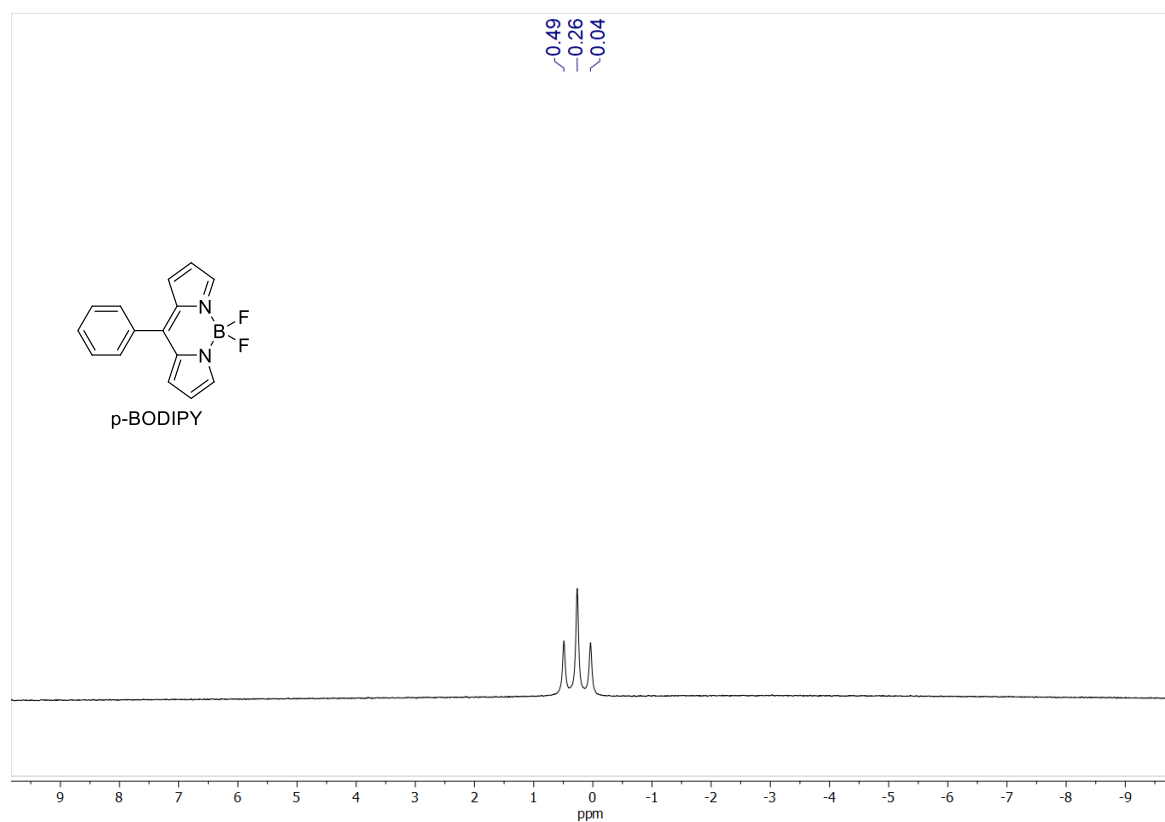


Figure S11. ¹¹B NMR spectrum of p-BODIPY in CDCl₃.